

# PHYSICAL MODELLING OF PROPELLER SCOUR ON AN ARMOURED SLOPE

by

*Neville Berard<sup>1</sup>, Sundar Prasad<sup>1</sup>, Brett Miller<sup>2</sup> and Mathieu Deiber<sup>2</sup>*

## ABSTRACT

CITIC Pacific Mining (CPM) is proposing to increase throughput at their existing terminal in Western Australia, using self-propelled Handysize transshipment shuttle vessels (TSV) instead of dumb barges. An initial assessment indicated that the armoured rock slope adjacent to the berth face would incur damage due to propeller wash from the vessel side thrusters and the main propeller. Large scale (13.5:1) physical model tests were undertaken at the University of New South Wales (UNSW) to measure wash velocity and armour stability. Empirical equations for propeller velocity along the axis well reproduced the bow and stern thruster velocities but could not match the profile of the larger main propeller measurements. Measurements made along the axis of the vessel bow thrusters were not affected by the operation of the second thruster, indicating that traditional equations for side by side propellers may overpredict velocities. Additionally, the physical modelling demonstrated that the rock slope was more stable than predicted, but still incurred the mobilization of a small amount of armour stone. Additional tests were then completed to investigate the efficacy of Articulated Concrete Block Mattresses (ACMs) to protect the rock slope from propeller wash. These tests showed that the mats performed well as additional protection on the armour slope but only if tied together to stop the edges from becoming dislodged and overturning.

## 1. INTRODUCTION

The CITIC Pacific Mining Sino Iron Magnetite project is located 100 km southwest of Karratha, in Western Australia and initiated commercial operation in 2013.



Figure 1: Aerial view of the Cape Preston facility showing a transshipment barge prior to the facility modifications. (Subcon, 2018)

---

<sup>1</sup> Ausenco, Canada, [neville.berard@ausenco.com](mailto:neville.berard@ausenco.com)

<sup>2</sup> UNSW Sydney, Water Research Laboratory, Australia

The facility, shown in Figure 1, was originally designed to berth transshipment barges with no propulsion capability. The berth was recently modified to enable berthing of larger self-propelled Transshipment Shuttle Vessels (TSV). Canada Steamship Lines (CSL) was engaged to modify and provide the TSV Donnacona to be fit for these operations. The vessel is equipped with a combination of bow and stern thrusters in addition to the main propeller for unassisted berthing and de-berthing. The propulsion arrangement for the Donnacona is shown in Figure 2, Figure 3 and summarized in Table 1.

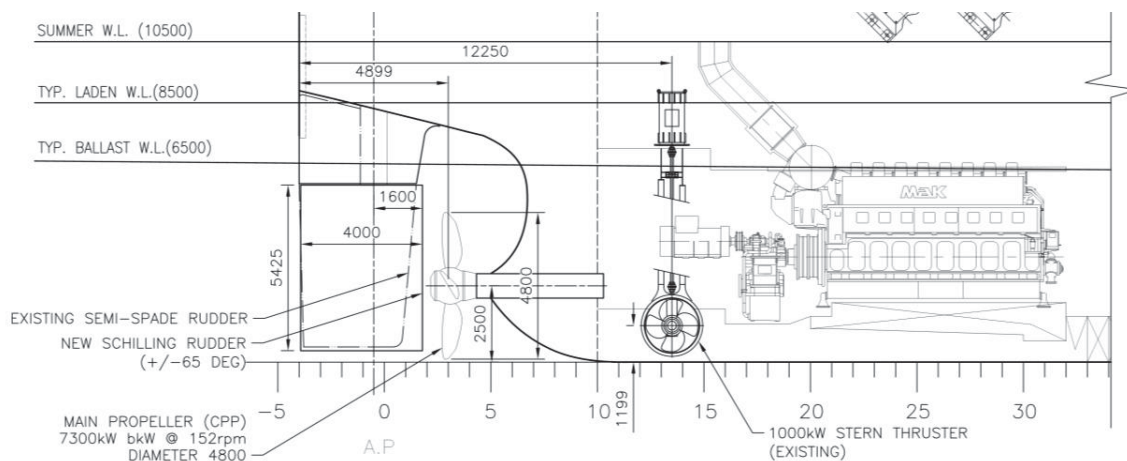


Figure 2: Donnacona stern propulsion arrangement

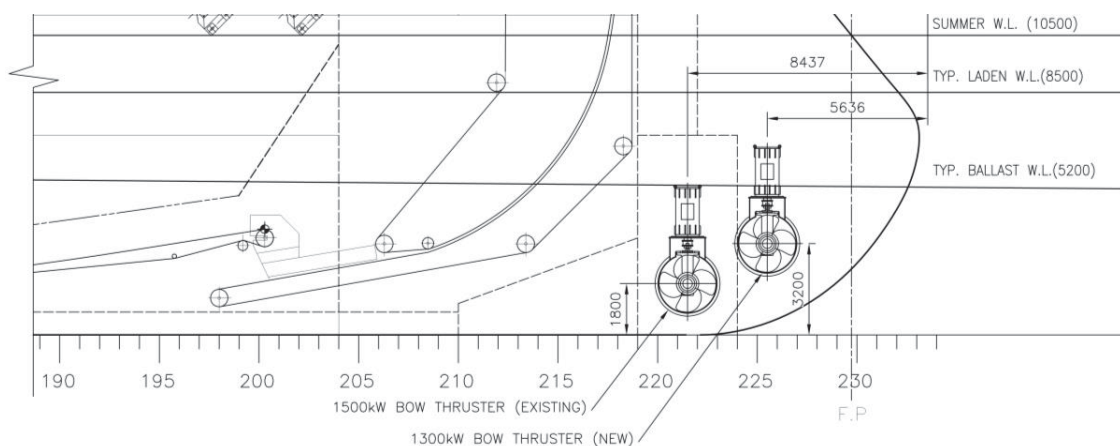


Figure 3: Donnacona bow propulsion arrangement

Table 1: Donnacona propulsions

Propeller	Diameter (m)	Power (kW)	Shaft Height above Keel (m)	Revolution (rpm)
Main Propeller	4.8	7300	2.5	152
Stern Thruster	1.75	1000	1.2	378
Bowthruster 1	2.0	1500	1.8	324
Bowthruster 2	2.0	1300	3.2	324

A desktop study was initiated because of concerns that the propulsion systems of the Donnacona could compromise the integrity of the armoured slope. Numerical calculations were performed following the latest guidance for slope stability by PIANC (2015) which includes three methods for the calculation of minimum rock weights for stability. All methods indicated that bow thrusters were likely to cause slope stability issues, but the three methodologies did not agree on whether the slope at the facility would be stable for the stern thruster and the main propeller.

A physical model study was determined to be the best method of reconciliation to confirm the findings of the numerical assessment and provide guidance on the stability of the armour stone at the terminal.

## 2. THEORETICAL BACKGROUND

The study of propeller velocities on slopes has gained more attention in recent years due to the increase in ship size and their respective propulsion systems. To determine the minimum diameter for stable armour, PIANC (2015) recommends two methods: the Dutch and the German formulations. Both methods involve two steps: the calculation of flow velocities produced by the propeller and then the subsequent calculation of armour stone to withstand those velocities. PIANC (2015) provides a warning that the two sets of equations for flow can vary significantly and therefore the corresponding equations (Dutch or German) for minimum diameter for stable armour stone should be used.

Recent physical model scale testing programs conducted by Dykstra et al. (2010) and van Doorn (2012) have contributed to the ongoing effort to better understand the velocities produced by propellers and their effect on the stability of armoured slopes.

### 2.1 Jet Velocity

Efflux velocity, the velocity of a jet along the central axis right at the propeller, was calculated according to Blaauw and Van de Kaa (1978):

$$V_0 = C_3 \left( \frac{f_p P_D}{\rho_w D_p^2} \right)^{0.33} \quad (1)$$

where  $C_3$  is 1.17 for ducted propellers or 1.48 for free propellers,  $f_p$  is the percent of total engine power,  $P_D$  is total installed power,  $\rho_w$  is the density of water and  $D_p$  is the propeller diameter.

The Dutch equation for flow distribution along the main propeller axis is determined according to:

$$V_x = (2.0 \text{ to } 2.8) V_0 \left( \frac{D_p}{x} \right) n \quad (2)$$

where  $x$  is the distance along the central axis from the propeller and  $n$  is the square root of the number of propellers. This equation is valid for  $x > 2.6 * D_p$ , called the zone of free propagation. When  $x < 2.6 * D_p$ ,  $V_x = V_0$  which is referred to as the zone of flow establishment.

The German equation is similar but instead of a range of values (2.0 – 2.8) as shown in (2), the equation applies a constant of 2.6.

$$V_x = (2.6) V_0 \left( \frac{D_p}{x} \right) n \quad (3)$$

For the velocity decay of the bow thruster jets (as opposed to main propeller jets) over a slope there is a German equation presented in PIANC (2015) method which was derived from physical model tests with a slope of 1V:3H.

$$V_x = V_0 \text{ for } \frac{x}{D_p} < 1 \quad (4)$$

$$V_x = V_0 \left( \frac{x}{D_p} \right)^{-0.33} \quad \text{for } 1 < \frac{x}{D_p} < 5.375 \quad (5)$$

$$V_x = 2.3V_0 \left( \frac{x}{D_p} \right)^{-0.825} \quad \text{for } \frac{x}{D_p} > 5.375 \quad (6)$$

## 2.2 Armour Stability

PIANC (2015) includes three separate methods for the determination of stable armour rock on slopes to withstand propeller velocities: The German method, the Dutch/Izbash method and the Dutch/Pilarczyk method. The German methodology is based on research and equations specifically for propeller jets while the Dutch methods use basic stability formulas developed by Izbash and Pilarczyk.

The German stability approach as it is shown in PIANC (2015) is

$$V_{crit} = B_{crit} \sqrt{D_{85} g \Delta} \quad (7)$$

where  $B_{crit} = 0.9-1.25$ ,  $g$  is acceleration due to gravity and  $\Delta$  is the relationship between stone density and the density of water ( $\rho_s - \rho_w / \rho_w$ ).  $V_{crit}$  is the critical velocity that mobilizes the armour stone and  $D_{85}$  is the diameter that 85% would pass through on a sieve test.

The Dutch/Izbash method uses the following equation:

$$\Delta D_{50} = \frac{1}{B_{crit}^2} \frac{V_{bottom}^2}{2g} \quad (8)$$

where, in this case,  $B_{crit} = 0.8$ ,  $V_{bottom}$  is described as the flow velocity near the bed and  $D_{50}$  is 50% passing diameter for armour stone.

Finally, the Dutch/Pilarczyk method from CIRIA, CUR, & CETMEF (2007) is:

$$\Delta D_{50} = \phi \frac{0.035 k_h k_t^2 V^2}{\psi_{cr} k_{sl} 2g} \quad (9)$$

where:

$\Phi$  = stability parameter (taken as 0.75 for riprap)  
 $\psi_{cr}$  = critical Shield's parameter (0.035 for riprap)  
 $k_h$  = depth parameter, 1.0  
 $k_t^2$  = turbulence factor, 3.0 from Pilarczyk (1990)  
 $\alpha$  = angle of internal friction (40° for riprap)  
 $\theta$  = revetment slope  
 $k_{sl} = \sqrt{1 - \left( \frac{\sin \alpha}{\sin \theta} \right)^2}$

All three of these equations were used during the initial desktop study and yielded significantly different results. For this reason it was unknown which of these methods provided the most realistic results and thus physical model testing was determined to be a more reliable method of determining the stability of the existing armour rock at the facility.

### 3. PHYSICAL MODEL SET-UP & TESTING

The physical model was constructed in a 4 m x 7 m x 1.4 m deep basin at the University of New South Wales' (UNSW) Water Research Laboratory. Both mobile and fixed bed tests were completed to understand if any observed instabilities were caused by undermining or armour rock instability.

Articulated concrete mattresses (ACMs) had previously been suggested as a solution should the armour stability not be sufficient. These mattresses were also tested in the lab to establish whether the selected mattresses could withstand the propeller velocities.

#### 3.1 Physical Model Layout

The features of the model (shown in Figure 4) were:

- A plywood slope upon which the breakwater was built with a slope of 2V:3H.
- A section of moveable bed with could be covered during fixed bed testing
- A propeller drive and motor for the different configurations
- A beam for supporting and moving the Acoustic Doppler Velocimeter (ADV).

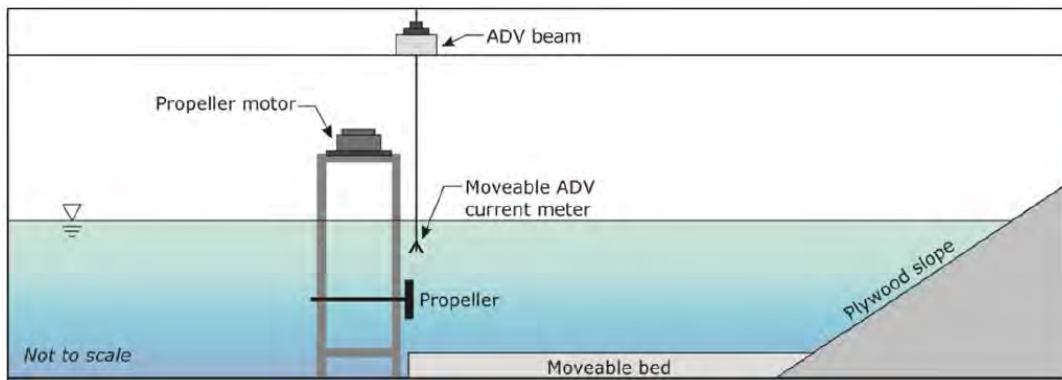


Figure 4: Model features – side view.

The modeling was undertaken at a Froude scale of 1:13.5. This scale was determined so as to:

- Maintain adequate turbulence for the rock stability testing;
- Provide adequate resolution and accuracy for model measurements
- Ensure the basin had enough space for water circulations and jet dispersion;

Propellers were affixed assuming a minimum underkeel clearance of 1.2 m to represent a worst case scenario. Testing set-up of the bow thrusters is shown in Figure 5.

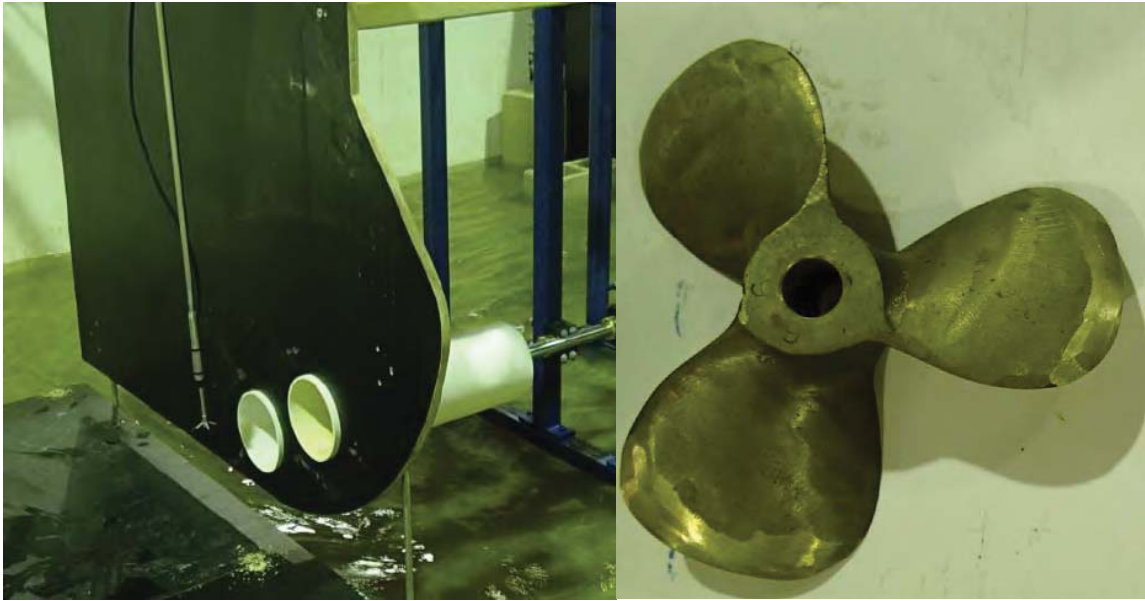


Figure 5: Bow thrusters installation with ADV probe (left) and view of a propeller used for a bow thruster (right)

Prototype armour rock had a median weight of 500 kg and was overlaid on a filter layer which sat directly on the plywood. The seabed at the site is composed of 10 mm rocks. For the mobile bed tests, this was modeled using a scaled mix of sand with diameters between 0.3 mm to 2 mm.

ACMs were modelled after mattresses produced by the manufacturer Subcon. The design for the laboratory prototypes was determined in consultation with them. ACMs were constructed with a density of  $2600 \text{ kg/m}^3$  and with an area density of  $521 \text{ kg/m}^2$ . Blocks were manufactured by injection mold in two interlocking sections. Model ACMs (shown in Figure 6) were assembled by aligning the blocks over string-lines and clicking the blocks into place.



Figure 6: Articulated concrete mattresses (as modelled)

A Nortek Acoustic Doppler Velocimeter (ADV) was used to measure velocities at the propellers during testing. A 3D FARO laser scanner was used to scan the breakwater and mobile bed (if applicable) before and after each test to assess any differences (see Figure 7). At the conclusion of each test the before and after images were compared using 3D point cloud software to determine if rock movement occurred. Rock movement was defined as when a rock moved more than the median rock dimension.

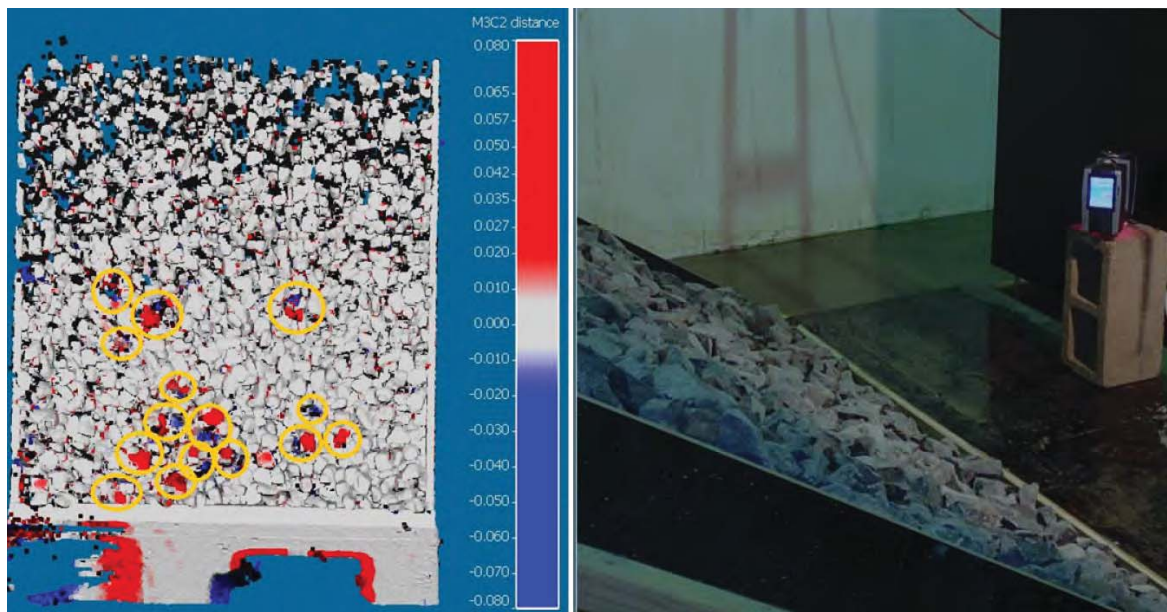


Figure 7: Example of a FARO Scan (left) and the FARO scanner in action in the laboratory

### 3.2 Testing Program

A description of all tests performed during these experiments is shown in Table 2. Engine power percentages were determined through discussions with the terminal operators, a simulation completed during a maneuvering study by the Australian Maritime College (2016) and using industry recommendations from PIANC (2015).

Mobile bed tests were designed to represent realistic operating conditions at the site. Fixed bed tests allowed the effect of the velocities on the armour rock slope to be isolated for the worst case scenario (minimum underkeel clearance) without any undermining of the slope occurring.

Tests were re-set (slope rebuilt, sand re-flattened or both) at the beginning of each major test series (numbered items in Table 2).

Each test was run for a period of 30 minutes prototype, which translated to approximately 8.5 minutes at the lab scale. This was selected to represent a number of ships calling at the facility and repeated velocities on the slope.

ACMs were used in the final test rounds as a proposed solution to erosion at the toe of the structure and instability of the armoured slope.

Table 2: Test program

Test #	Propulsion Type	Propeller Power (%)	Fixed or Mobile Seabed	Articulated Concrete Mattress
1a	Bow Thrusters	40	Fixed	No
1b	Bow Thrusters	70	Fixed	No
1c	Bow Thrusters	100	Fixed	No
2a	Bow Thrusters	40	Mobile	No
2b	Bow Thrusters	100	Mobile	No
3a	Main Propeller	30	Fixed	No
3b	Main Propeller	70	Fixed	No
4a	Main Propeller	30	Mobile	No
4b	Main Propeller	70	Mobile	No
5a	Main Propeller + Stern Thruster	30/100	Fixed	No
5b	Main Propeller + Stern Thruster	70/100	Fixed	No
6a	Main Propeller + Stern Thruster	30/100	Fixed	Yes
6b	Main Propeller + Stern Thruster	70/100	Fixed	Yes
7a	Bow Thrusters	40	Fixed	Yes
7b	Bow Thrusters	70	Fixed	Yes
7c	Bow Thrusters	100	Fixed	Yes

## 4. DISCUSSION & ANALYSIS

### 4.1 Jet Velocity

Data on efflux velocities for the Donnacona propulsion system was not available so (1) was used to convert engine power and propeller diameter to efflux velocities. The calculated velocities for various engine powers are shown in Figure 8. From this plot, the laboratory model propellers were calibrated to produce the desired velocity output for the simulated engine percentages required for the test program (see Table 2).

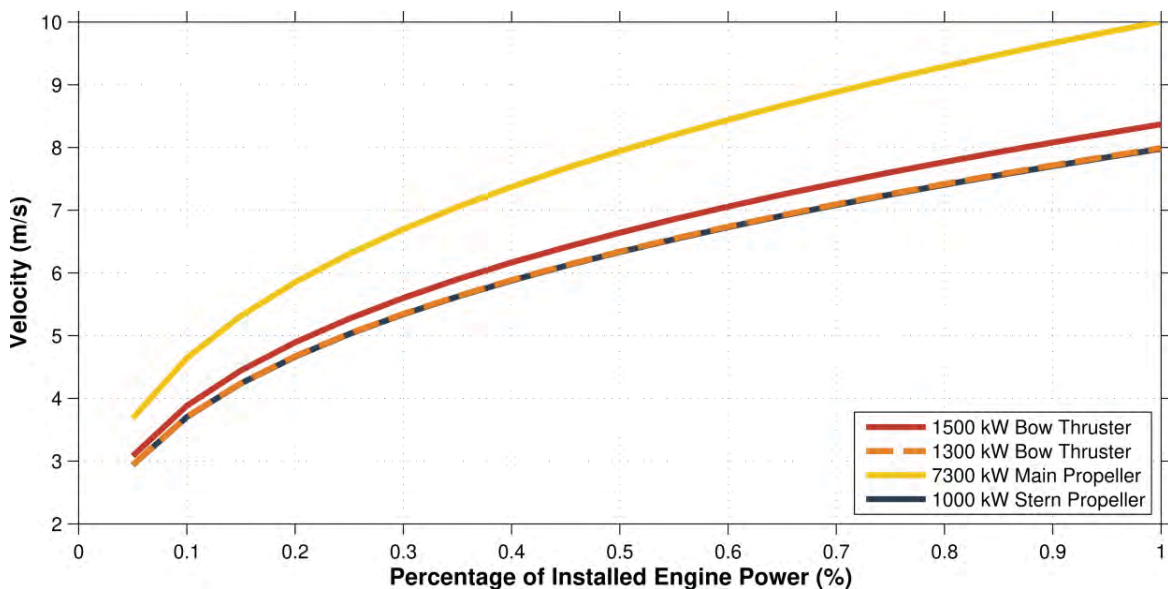


Figure 8: Calculated theoretical efflux velocities for the Donnacona propulsion systems



Once efflux velocities had been calibrated, the decay of the velocity along the propeller axis was measured for the main propeller, bow thrusters and the stern thruster. The ADV measured velocities were post processed by the program WinADV (Wahl, 2000) by applying the “Phase-space threshold despiking” method from Goring & Nikora (2002). An error value for each velocity measurement was calculated on the post-processed time series as per:

$$x_{rms} = \sqrt{\frac{1}{n}(x_1^2 + x_2^2 + \dots + x_n^2)} \quad (10)$$

where  $x_{rms}$  is the root mean square of the data (shown as the error bars in the plots below),  $n$  is the total number of values in the time series and  $x_n$  is each value in the time series.

These decay measurements were then able to be compared to the available empirical equations from PIANC (2015).

In the case of the main propeller (see Figure 9) the measured velocities were compared to the Dutch Equation (2) and the German Equation (3). The minimum value of the Dutch equation (coefficient from (2) equal to 2.0) is taken to get the best agreement with the data. No guidance is provided in PIANC (2015) on how values between 2.0 to 2.8 for equation (2) should be selected when using this equation. In both cases, the measurements decreased significantly quicker than what was predicted by the equations. The length of the zone of flow establishment, where the efflux velocity is constant, appears to be significantly overpredicted by both methods.

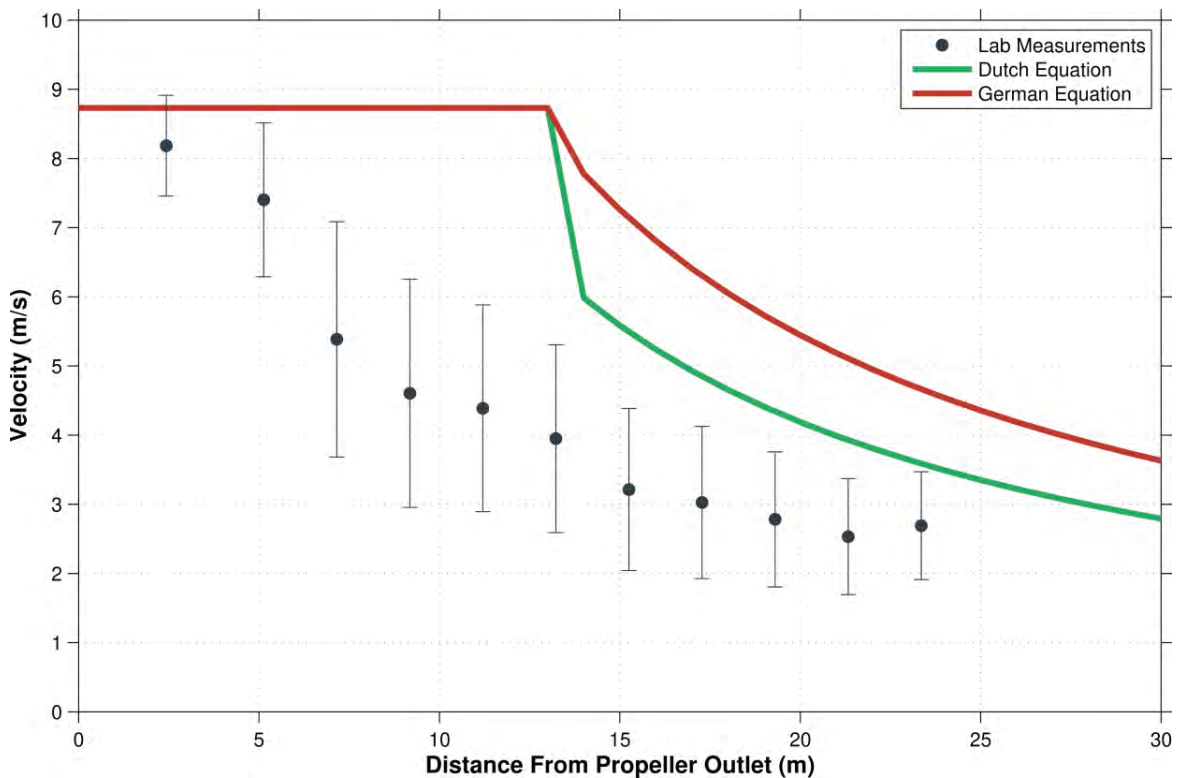


Figure 9: Main Propeller velocity decay profile compared with empirical equations

For the bow thrusters (Figure 10), tests were performed with a single thruster operating and with both thrusters operating. All measurements were taken along the centerline of the lower bow thruster. It is important to note that predicted flow velocities for the case with 2 propellers running would apply between the two axes. In the physical model tests velocities along the centerline of the lower bow

thruster were not influenced by the operation of the second thruster (shown as very little change in the two measurement cases in Figure 10). It is suggested that the equation for two bow thrusters is not relevant and would likely not be representative of many scenarios, especially as it considers that flows increase by the square root of the number of propellers. In this scenario that factor is 1.4 which does not appear to be realistic. More tests would be required to confirm this. The single thruster Dutch equation provides a better approximation but slightly under predicts the velocities at a distance of approximately  $4 \cdot D_p$ .

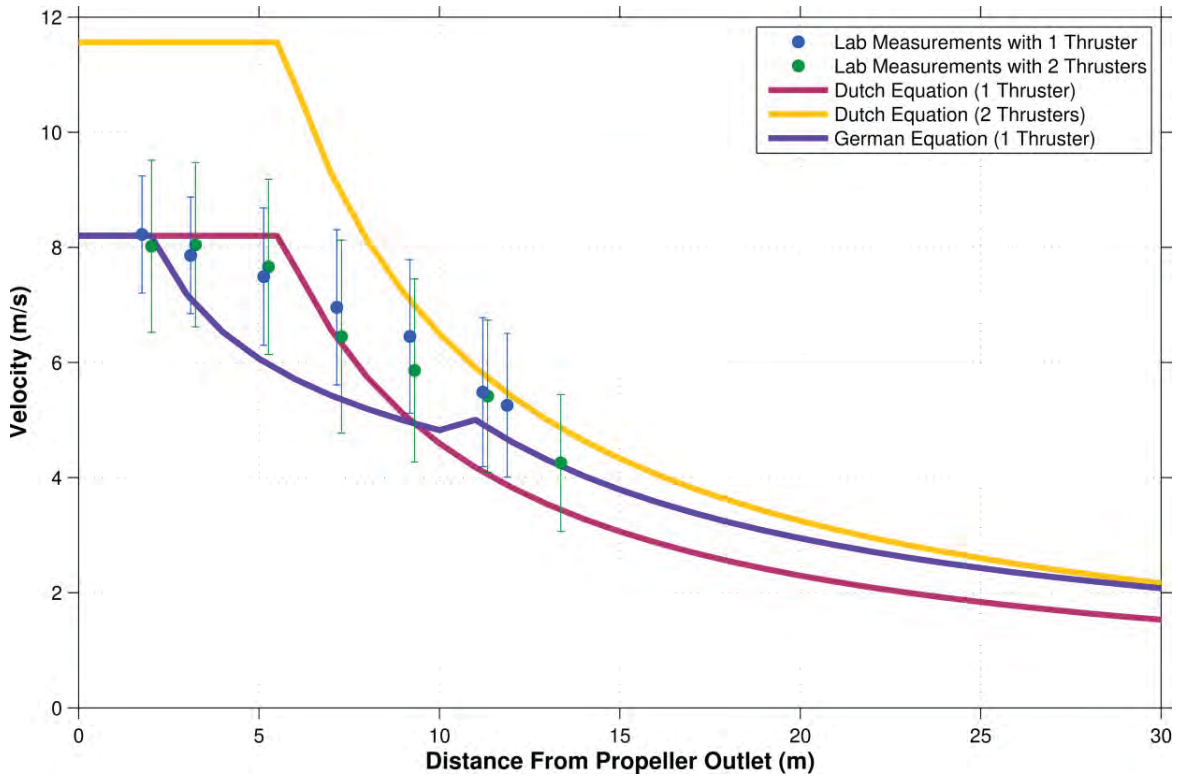


Figure 10: Bow thrusters velocity decay profiles compared with empirical equations

For the stern thruster model tests, a non-ducted propeller was implemented instead of a ducted propeller in order to achieve the desired velocities during the calibration phase. The velocity decay curve is shown in Figure 11 and compares well with both the Dutch and the German equations assuming ducted propellers ( $C_3 = 1.17$  in equation (1)). The Dutch equation appears to provide the overall best representation of the flow in this instance.

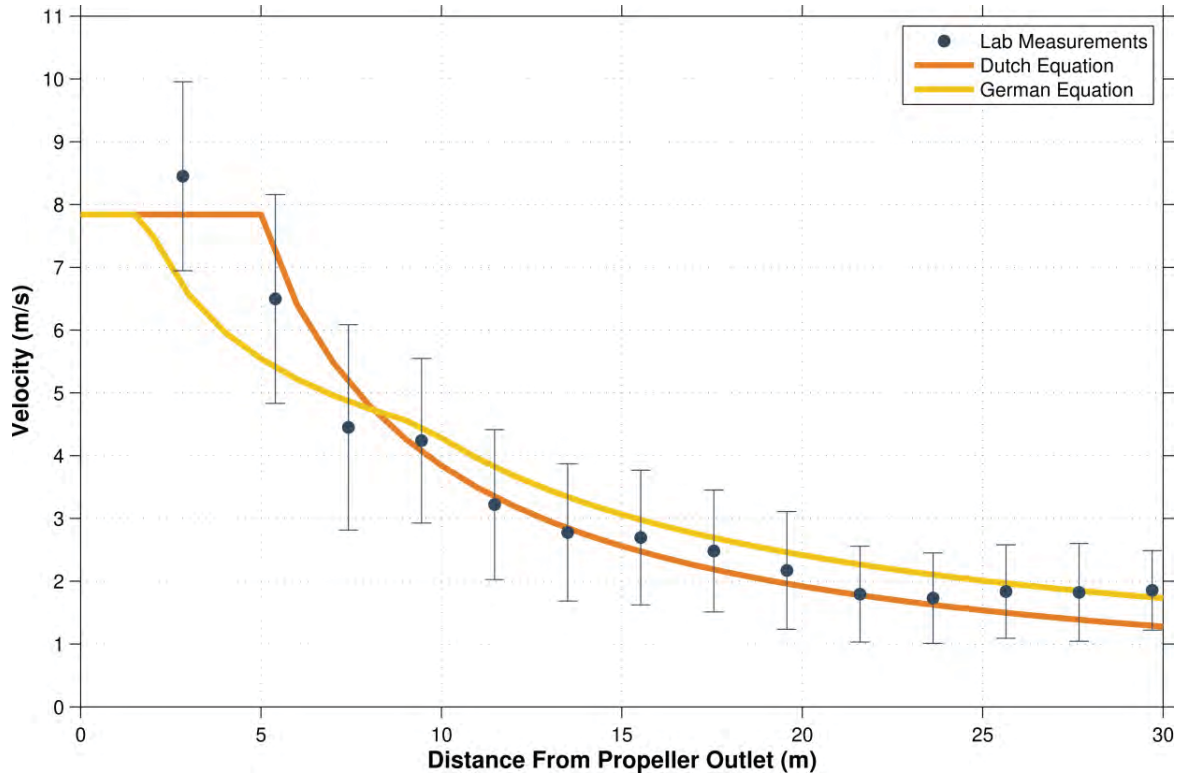


Figure 11: Stern Thruster velocity decay profiles compared with empirical equations

#### 4.1 Armour Stability

Stability was determined mainly using the results of the FARO scan system described above in Section 3.1.

##### 4.1.1 Mobile Bed Tests

Due to the low underkeel clearances considered for this study and the fine sediment native to the berth area, scouring of sediment from underneath the armour slope was the primary failure method throughout all mobile bed tests. During the mobile bed tests significant movement was observed for sediment in front of both bow thrusters (Test 2) and the main propeller (Test 4) during all test scenarios. In all cases this resulted in localized failure of the armour rock slope. An example of the results from Test 2b (bow thrusters in extreme conditions with 100% power) is shown in Figure 12 and Figure 13.

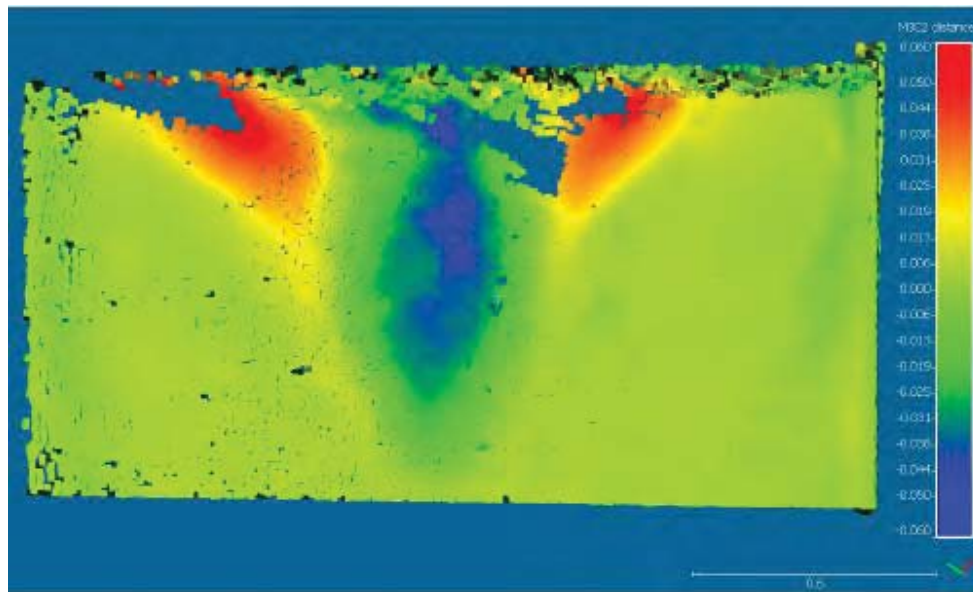


Figure 12: FARO scan results of Test 2b showing show scour hole formation.



Figure 13: Photo of Test 2b scour hole formation

#### 4.1.1 Fixed Bed Tests

Rock movement was observed in all fixed bed tests performed without ACMs. A summary of rock movement is provided in Table 3.

Table 3: Rock movement observed during fixed bed tests

Test series	Test	Rocks Moved
1	a	5
	b	18
	c	23
3	a	2
	b	6
5	a	3
	b	13

Examples of the FARO post-processed scans with rock movement identified are shown in Figure 14 and Figure 15.

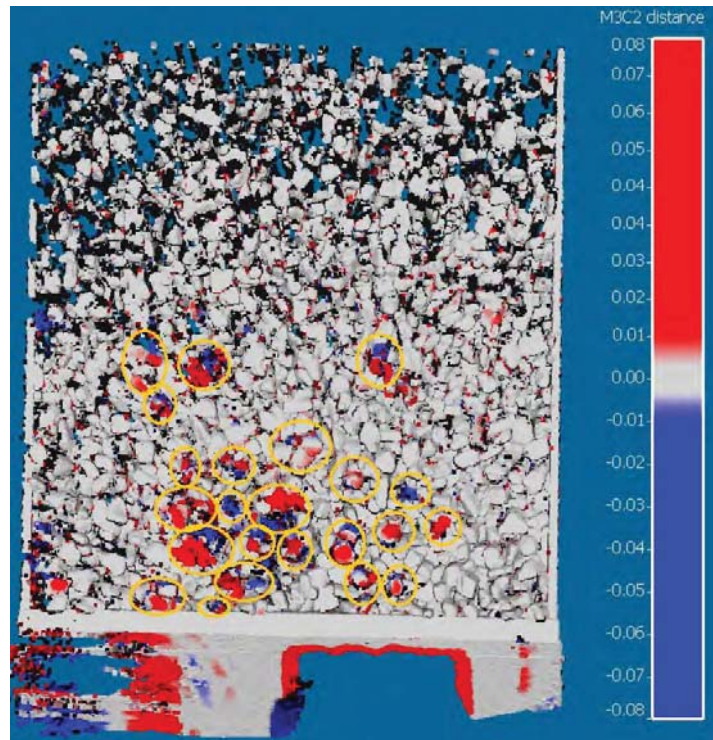


Figure 14: FARO scan at the conclusion of Test 1c. A total of 23 rocks (circled in yellow) moved.

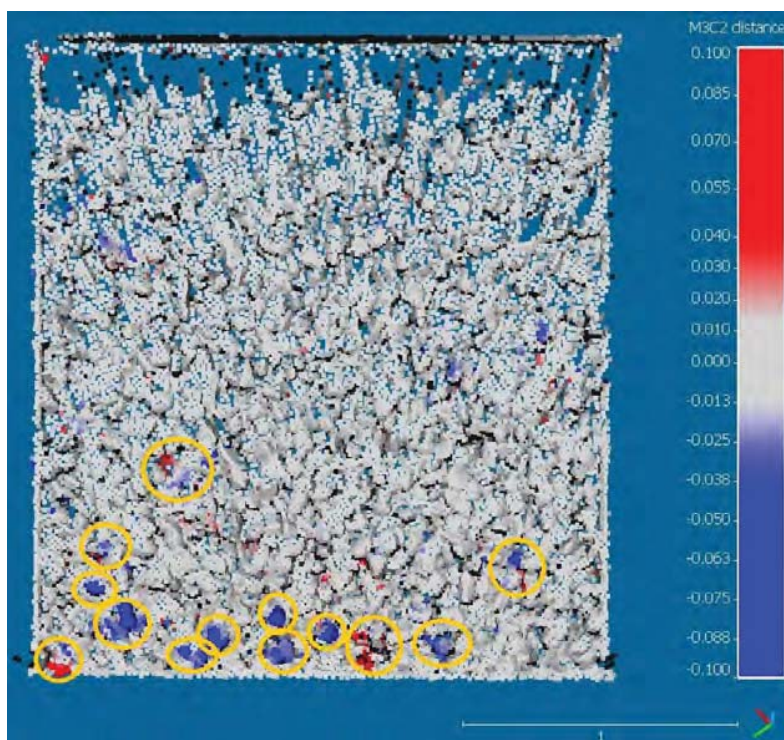


Figure 15: FARO scan at the conclusion of Text 5b. A total of 13 rocks (circled in yellow) moved.

Test results for the bow thrusters during the fixed bed tests showed rock movement outside of the expected wash zone of influence (assuming a 10 degree spread nominally associated with the wash plume). It was assumed that this was due to the rock slope effects, but could also be attributed to the impermeable core (plywood board) used in this model. More testing is required to determine if this pattern is consistent in similar tests. This was important when considering the design limits for additional slope protection such as ACMs.

Using the decay measurements conducted for the propellers (see Figure 9 and Figure 10) an approximate value of the velocity at the slope along the propeller axis was determined. This resulted in  $V = 2.5 \text{ m/s}$  @ 25 m from the main propeller outlet and  $V = 4.0 \text{ m/s}$  at 14.5 m from the bow thruster propeller outlet. These velocities were used in Equations 7, 8 and 9 to determine what stable rock weights would have been calculated. A stone density of  $2700 \text{ kg/m}^3$  was used to replicate the laboratory conditions. For equation 7, a ratio of  $D_{50} = D_{85}/1.25$  was used to allow the comparison between all three equations.

Resulting rock weights (shown in Table 4) were then compared with the physical model test results (Table 3). Test 1c was the extreme case for the bow thruster scenario which is assumed to be representative of unstable armour slope conditions (23 total rocks moved). Test 3b was the extreme scenario for the main propeller testing which saw limited rock movement and was marginally unstable.

Table 4: Predicted stable rock weights for each stability equation

Wash Source	Required Rock Weight, $W_{50}$ (kg)		
	German	Dutch/Izbash	Dutch/Pilarczyk
Main Propeller	21 - 155	75	1,770
Bow Thrusters	360 - 2,585	1,280	29,700

The German methodology provided a wide range of values when using the recommended  $B_{crit}$  (0.9-1.25) values. With  $B_{crit} = 1.25$ , rock sizes are clearly under predicted ( $W_{50} = 21$  and 360 for main propeller and bow thrusters respectively). Using  $B_{crit} = 0.9$  resulted in the stable rock weight for the main propeller being too small (155 kg) but the bow thruster recommended weight of 2,585 kg is likely a realistic value.

Similarly, the Dutch/Izbash equations underpredict the rock sizes for the lower main propeller velocity but propose a reasonable 1,280 kg for bow thruster protection. Both of these methods (German and Dutch/Izbash) require more research into why reasonable values for protection are only produced at higher velocities. More guidance is also needed on the wide range of values proposed in PIANC (2015) for the  $B_{crit}$  constant in the German equation.

Finally, the Dutch/Pilarczyk method has significantly higher values for both propulsion methods. In this case the main propeller stable armour weight is of a reasonable scale (~1.8t) while the bow thruster armour weight is not. This equation has a significant amount of parameters and the guidance provided in PIANC (2015) could be further refined to improve its predictive ability

Overall, all three equations predict a significant increase in weight for a velocity increase of 1.5 m/s. More testing is required to determine if there is an optimal velocity range that some of these equations work well for or if the equations require modification when being used with actual velocity values, as opposed to predicted velocities output by equations 1 – 6.

#### 4.1.2 Articulated Concrete Mattresses

For Test 6 and Test 7 ACMs were placed on the slope and secured at the top using their cables. They extended 2.7 m from the toe of the armour slope (approximately 6 square units)

For Test 6 the ACMs were secured only from the top of the slope in order to see if the weight of the mattresses alone was sufficient to add protection to the slope. After both of the tests in the series, progressive flipping of the mats was observed which made them ineffective. An extreme example of the flipping that occurred from Test 6b is displayed in Figure 16 .

For the final test, the mats were tied together at the toe and mid way up the slope to see if this would remove the flapping and subsequent flipping of mattresses observed during Test 6. During Test 7, some flapping was observed during the actual testing but no movement was documented by the scan at the ending of the test as seen in Figure 17.

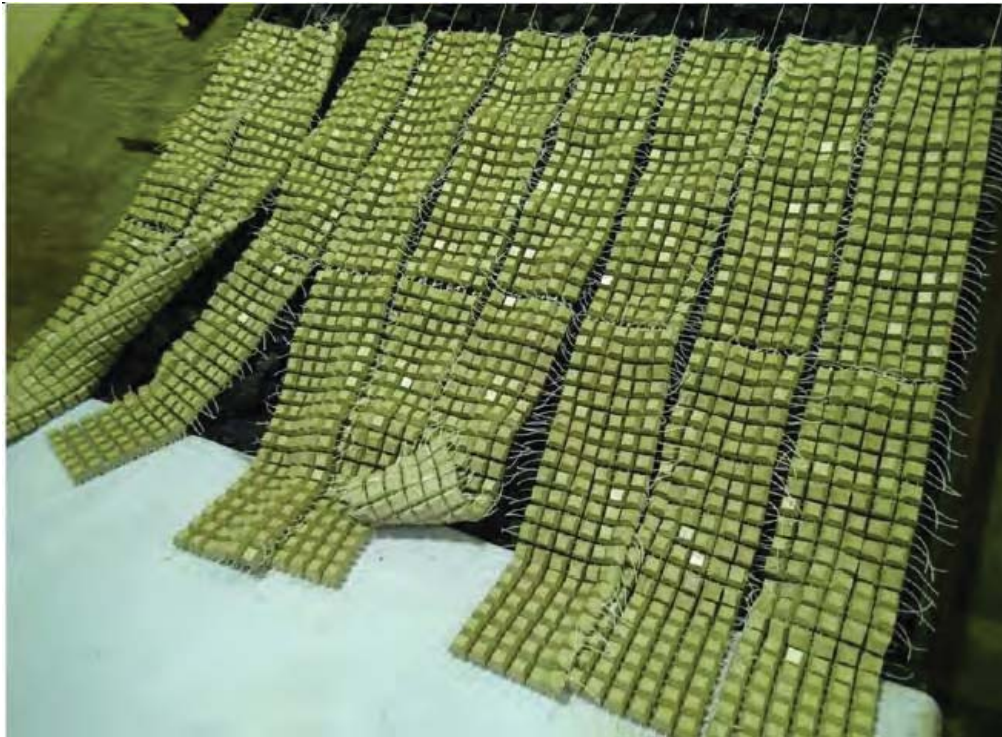


Figure 16: Armoured slope with ACMs after the conclusion of Test 6b.

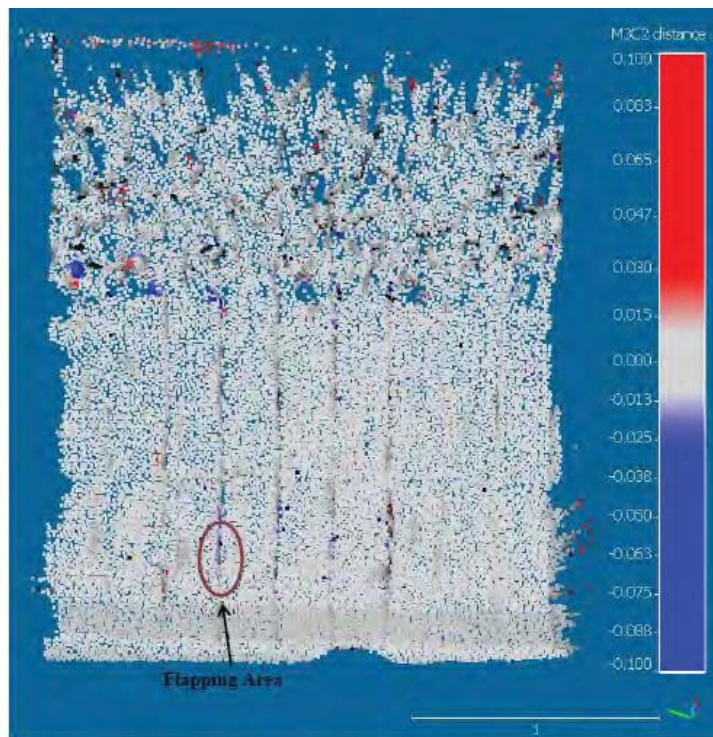


Figure 17: FARO scan at the conclusion of Test 7b.



## 5. CONCLUSION

A series of physical model tests were performed to better understand the effects of the TSV Donnaconna's propulsion system on an armour slope during the berthing process. Over the course of these tests, measurements of the decay of velocities as a function of distance from the propeller provided the following conclusions:

- For all three propeller type tests, velocities were seen to drop sharply with distance from the propeller. This leads to the conclusion that the zone of flow establishment which is typically valid for  $2.6 \cdot D_p$  may not be representative for large propellers;
- In addition to the over prediction of the zone of flow establishment, both the Dutch and German equations significantly over predicted the velocities with increasing distance from the main propeller jet;
- When measuring along the centerline of a one bow thruster jet there was no increase in velocity along the propeller axis when the second jet was operational. The modification of equation (2) for two jets is likely conservative, especially in the zone closest to the propeller outlet. This supports the findings of Dykstra et al. (2010) who came to similar conclusions; however, more tests are needed to determine if the results are the same for different bow thruster arrangements.
- The Dutch equation (2) provided the best approximation of flow decay for all three test cases in these physical model experiments.

Measurement of armour rock stability during fixed bed tests provided the following conclusions:

- During the operation of the bow thrusters, rock movement was witnessed outside of the expected zone of influence (assuming a 10% spread of the jet). This is likely due to the effects of the rock slope and should be considered when providing additional protection to slopes in the zones of influences of thrusters;
- Articulated Concrete Mattresses were found to be effective at stabilizing the velocities produced by the propulsion system only if tied together at the toe and top of the slope. For real world applications it is recommended that the ACMs should be connected along their full length to neighbouring mats;
- More testing is required to understand and refine the equations from PIANC (2015) sizing rock for armour stability. Calculations for measured velocities show that the German and the Dutch/Izbash equations provide reasonable estimates of stable rock sizes at higher velocities produced by bow thrusters but under predicted rock sizes for a propeller velocity of 2.5 m/s. The Dutch/Pilarczyk predicted significantly higher velocities than the other equations but also had a significant discrepancy between the two velocities tested. More research is needed to refine and understand the use of these equations with measured velocity values.

Based on the results presented herein, equations used to predict propeller wash velocities and subsequent stable armour rock are highly variable and require further research. For these reasons scale physical models are recommended to determine and test suitable armour protection for vulnerable slopes at port facilities.

## ACKNOWLEDGMENTS

Generous thanks to Nathan Fuller from CITIC Pacific Mining for enabling this contribution.

## REFERENCES

Australian Maritime College (2016). CSL Shipping: Cape Preston Donnacona Simulations.

Blaauw, H.G., and van de Kaa, E.J. (1978). Erosion of bottom and sloping banks caused by the screw race of manoeuvring ships. Delft Hydraulics Laboratory, publication no. 202.

CIRIA, CUR, CETMEF (2007). "The Rock Manual. The use of rock in hydraulic engineering". 2<sup>nd</sup> Edition.

Dykstra, D., Tschirky, P., Shelden, J., & Cornett, A. (2010) Physical Model Tests of Bowthruster Impacts on Armored Slopes. Ports 2010.

Goring, D.G., and Nikora, V.I. (2002). Despiking Acoustic Doppler Velocimeter Data. Journal of Hydraulic Engineering, 128(1), 117-126.

PIANC (2015). Report No 180, Guidelines for Protecting Berthing Structures from Scour Caused by Ships, PIANC, Brussels.

Pilarczyk, K. (1990). "Coastal Protection". Proc. of a short course, published by A.A. Balkema, Rotterdam.

Subcon (2017). Subcon awarded sino iron project for manufacture & supply of concrete scour mattresses. November 3, 2017. [www.subcon.com](http://www.subcon.com).

van Doorn, R. (2012). Bow thruster currents at open quay constructions on piles. Master's Thesis from Delft University of Technology, Delft, The Netherlands.

Wahl, T. (2000). Analyzing ADV Data Using WinADV. 2000 Joint Conference on Water Resources Engineering and Water Resources Planning & Management. Minneapolis, Minnesota.